AXIAL LOADS ACTING ON MANDREL IN COPPER RIFLED TUBE DRAWING PROCESS①

Peng Dashu, Yang Bin, Wang Feiyong, Yang Linbin
Department of Materials Science and Engineering,
Central South University of Technology, Changsha 410083

ABSTRACT Stresses and axial loads acting on the mandrel in the copper rifled tube drawing process were analysed, and factors affecting on the axial loads on mandrel were discussed. Results show that the depth of the mandrel dragged into sizing zone and lubrication have major influence on drawing loads and fin shapes.

Key words drawing copper rifled tube lubrication fin

1 INTRODUCTION

In recent years, the rifled tube, i. e. a tube with spiral groove on its inner surface, is developed. The rifled tubes are widely used in heat exchangers of air conditioners and refrigerators because of their excellent heat transfer performance, compared with that of conventional copper bare tubes[1-3]. The rifled tube drawing is different from the conventional bare tube drawing in the mandrel itself rotating in the drawing process (see Fig. 1). Up to date, however, the analysis of axial loads on rotating mandrel has not been reported. In this paper, stresses and axial loads acting on the mandrel in the rifled tube drawing process were analysed and factors affecting on the axial loads on mandrel were discussed.

2 ANALYSIS

Fig. 2 shows external forces acting on the mandrel in the rifled tube drawing process. In order to analyse stresses acting on the mandrel, the following assumptions are made.

(1) The inner surface of the drawing tube are gradually contacted with the driving side of grooves of the rotating mandrel in the drawing process.

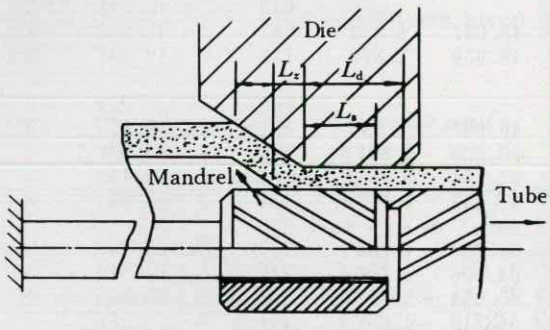

Fig. 1 Schematic illustration of the rifled tube drawing with spiral groove mandrel

(2) The normal pressure of the contacted side between the drawing tube and the groove is appoximately p_r.

(3) The circumferential component p_t of p_r constitutes the driving moment of the rotating mandrel in the drawing process.

(4) The resistant moments are constituted from friction stresses and so on. It is shown in Fig. 2 that

$$\left.\begin{aligned} &p_n = p_r \times \cos\gamma,\ p_b = p_n \times \cos\varphi, \\ &p_t = p_n \times \sin\varphi,\ p_b' = \mu \times p_n \times \cos\varphi, \\ &p_t' = \mu \times p_n \times \sin\varphi \end{aligned}\right\} \quad (1)$$

where γ —groove top angle; φ —helex an-

① Received Apr. 24, 1995; accepted Sep. 15, 1995

gle; μ —friction coeffcient.

On basis of moment equilibrium of the rotating mandrel, it follows that

$$p_t \times S_3 \times r = (p_t' \times S_3 + \mu \times p_r \times S_2) r \quad (2)$$

where $S_3 = K_3 \times N_z \times H_z \times L_z$ —side contact area between the dirving side of the groove and the inner surface of tube; $S_2 = K_2 \times \pi \times D_x \times L_z$ —contact area between the top of the groove and the inner surface of the tube; $K_2 (< 1)$ —ratio of contact in S_2; $K_3 (< 1)$ —ratio of contact in S_3; N_z —number of grooves; H_z —depth of groove; L_z —length of contact in the deformation zone; D_x —mean diamenter of the drawn tube.

Substituting eqs. (1) into (2), then

$$P_b = p_r \times [\mu/(\mathrm{tg}\varphi - \mu)] \times (S_2/S_3) = \mu' \times p_r \quad (3)$$

where

$$\mu' = [\mu/(\mathrm{tg}\varphi - \mu)] \times (S_2/S_3) \quad (4)$$

On the basis of analysis of the forces acting on the mandrel in Fig. 2, the axial forces acting on the mandrel have P_b, P_b', $\mu \times P_r \times \sin\gamma$ and $\mu \times P_r \times S_4$, thus the axial load acting on the mandrel is obtained

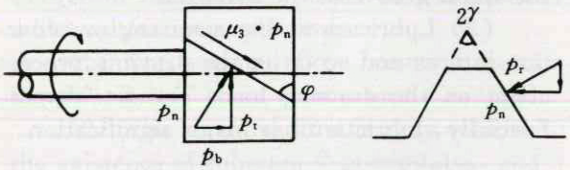

Fig. 2 Schematic representation of stress distribution in the mandrel

$$P_x = (P_b + P_b') \times S_3/\mathrm{tg}\varphi + \mu \times P_r (S_2 + S_4) = P_r[(\mu' + \mu \times \sin\varphi/\sin\gamma) S_3/\mathrm{tg}\varphi + \mu(S_2 + S_4)] \quad (5)$$

where $S_4 = \pi \times D_x \times L_s$ —contact area between the mandrel and the inner surface of the tube in the sizing zone; L_s —length of the mandrel draged into sizing zone.

The drawing load in the deformation zone is[4]

$$P_C = \frac{\sigma_t \times (1 + B)}{B} \times \{1 + \frac{t_2}{t_2}[\frac{B \times \sigma_{za}}{\sigma_t \times (1 + B)} - 1]\} \times S \quad (6)$$

and

$$P_r = \frac{t_1^{(1+B)} - t_2^{(1+B)}}{t_1 - t_2} \times (1 - \frac{B \times \sigma_{za}}{1 + B} + \frac{\sigma_t}{\mathrm{B}})/t_1^B \quad (7)$$

where $B = (\mu + \mu')/\mathrm{tg}\alpha$; α —die semi-angle; σ_{za} —stress on exit in tube drawing[4].

The drawing load acting on the sizing zone is

$$P_D = P_b \times S_4 \quad (8)$$

From eqs. (8) and (9), the drawing load is as follows:

$$P = P_C + P_D \quad (9)$$

3 EXPERIMENTAL

The annealed pure-copper bare tube of O. D. 9.52 mm and I. D. 8.72 mm is drawn into the rifled tube of O. D. 8.0 mm and I. D. 7.28 mm by tube drawing with fixed, spirally grooved mandrel. The rifle tube drawing are carried out with type WD-10 mechanical machine by the fixed, spirally grooved mandrel, of which the groove length is 2 mm, helex angle is 21°. The die semi-angle is 12°. The drawing load and axial loads acting on the mandrel are measured with strain gauges at the same time.

4 RESULTS AND DISCUSSION

Fig. 3 shows typical loads versus grips displacement curves for rifled tube with fixed mandrel. Fig. 4 shows influence of L_s on the drawing loads. Tables 1 and 2 show effect of L_s on the spiral raising angle (φ_s) on tube inner surface and effect of friction on drawing loads.

It is shown in Fig. 4 that the deeper (L_s) the mandrel draged into sizing zone, the higher the drawing loads because of increasing friction stresses in the sizing zone. So the site (L_s) of the mandrel in the sizing zone must be suitable. Otherwise, when L_s is excessive, the tendency of breakage in drawing tube increases; Or when L_s is too short, the fin shape of the tube may not fill into the spiral groove of the mandrel. Besides, lubrication, die an-

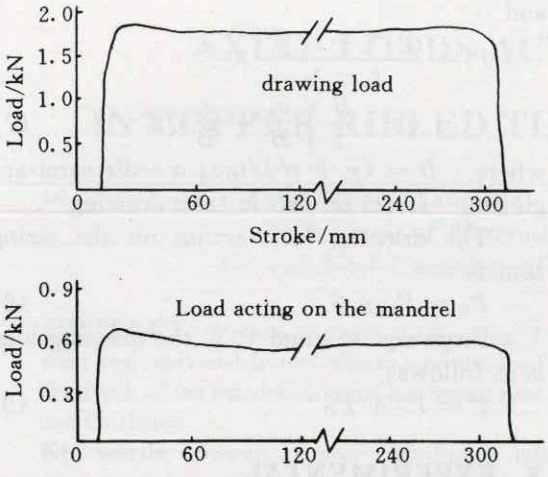

Fig. 3 Typical loads versus grips displacement curves for rifled tube with fixed mandrel

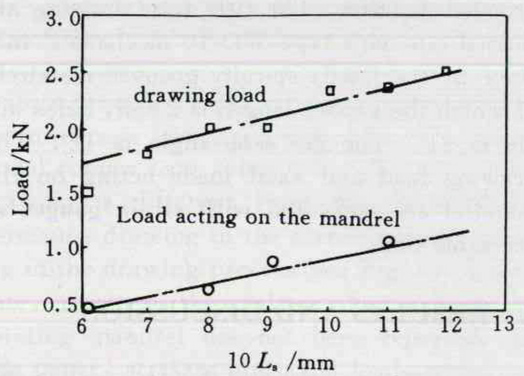

Fig. 4 Effect of L_s on drawing loads

Table 1 Effect of L_s on the spiral raising angle

No.	1	2	3	4
L_s /mm	1.1	0.7	0.9	0.8
φ_s /(°)	18.43	18.00	19.43	18.60
H_z /mm	0.11	0.07	0.08	0.08
No.	5	6	7	8
L_s /mm	1.2	0.5	1.0	1.1
φ_s /(°)	24.56	10.60	21.82	21.80
H_z /mm	0.12	0.05	0.09	0.11

Table 2 Effect of friction on drawing loads

Drawing	L_s /mm	Lubrication condition	μ^*	P /N	H_z /mm
d 9.5 mm ×0.40 mm	1.1	dry	0.16	2650	0.06
		mixed	0.12	1950	0.07
d 8.0 mm ×0.36 mm		wet	0.08	1400	0.10

μ^* —reference value of friction coeficient[5]

gle, reduction in area and so on in the drawing process affect on the drawing loads and fin shapes. Specially, lubriction has major signification (see Table 2).

5 CONLUSIONS

(1) The depth (L_s) of the mandrel draged into sizing zone and lubrication have major influence on drawing loads and fin shapes.

(2) The site (L_s) of the mandrel in the sizing zone must be suitable. Otherwise, when L_s is excessive, the tendency of breakage in drawing tube increases; or when L_s is too short, the fin shape of the tube may not fill the spiral groove of the mandrel.

(3) Lubrication, die semi-angle, reduction in area and so on in the drawing process affect on the drawing loads and fin shapes. Specially, lubriction has major signification.

REFERENCES

1 Iwao Takai *et al*. Simitomo Metals, 1982, 34(1): 136−143.

2 Shigeo Lijima *et al*. Technical Reports of Simitomo Light Metals, 1994, 35(1, 2):

3 Guan Xiaojuan. Copper Fabrication, (in Chinese), 1993, (2): 69−73.

4 Li Lianshi. Principle of Deformation in Steel Tubes, (in Chinese). Beijing: Metallurgical Industry Press, 1989: 4.

5 Yao Ruohao. Frication and Lubrication in Metal Forming, (in Chinese). Beijing: Metallurgical Industry Press, 1990: 10.

(Edited by Peng Chaoqun)